Supplement of The Cryosphere, 14, 1519–1536, 2020
https://doi.org/10.5194/tc-14-1519-2020-supplement

The Cryosphere Open Access EGU

Supplement of

An enhancement to sea ice motion and age products at the National Snow and Ice Data Center (NSIDC)

Mark A. Tschudi et al.

Correspondence to: Mark A. Tschudi (mark.tschudi@colorado.edu)

S1. Evaluation of uncertainties in source data motion estimates

The number and types of individual sources have changed over the ice motion product time series. Each source has different error characteristics based on the source and the method to estimate motion. As noted in the main text, Section 2.2, there have been several studies of motion estimate uncertainties, most focused on passive microwave motions derived from SSMI/SSMIS and AMSR-E imagery. These evaluations have been done via comparisons with buoy estimates. Buoy position is known very precisely and thus displacement and motion can be accurately retrieved. Thus, buoys act as a source of the "true" motion for validation.

Such comparisons were done early on in the product development and were used to derive the relative quality of the different source – i.e., the values of C in Equation 1. These C values have been used since without change. Here we provide a brief analysis of the source data via comparison with buoy source. This is not intended to be a complete validation study of each of the source motions. It is meant to give users of the product a general sense of the accuracy of the source motions.

The comparison method used all valid buoy motions over the given time period. For each buoy, the closest source motion estimate was found with a limit of 50 km (only source observations within 50 km of the buoy) were included. The u-component and v-component of motion, on the EASE grid, were compared between the source and the buoy for each day. All comparisons over the time period were used to calculate a bias (mean difference, e.g., $u_{\text{source}} - u_{\text{buoy}}$) and an Error Standard Deviation (Table S1). For each source, a typical year was chosen and statistics were calculated for winter (January through March) and summer (June through August). Particularly for the microwave estimates, this represents a period of optimal performance (winter) and a period with low performance (summer). For SMMR, summer estimates were very limited and there was not a large enough sample to effectively calculate statistics, so only winter is provided.

Overall, the statistics recapitulate what has been shown in previous studies. Passive microwave estimates generally have higher errors than AVHRR because of the lower spatial resolution. And spatial resolution of the source passive microwave imagery is a key factor in the error; higher spatial resolution imagery have lower Error Standard Deviation values. Note that SMMR Error

Standard Deviation values are relatively low because SMMR imagery is every other day and the daily value is a result of averaging between days, which reduces the noise in motion estimates.

One feature that is noticeable is the high errors in SSMI during summer, particularly the bias. This is not surprising given the difficulties in retrieving surface properties during the melt season. This perhaps argues against inclusion of SSMI (and SSMIS, which has similar characteristics) in the combined product during summer. However, the approach used in the product is to use all available inputs throughout the year. During summer, the number of vectors is lower, particularly for 85 GHz, so the impact of these lower quality vectors is relatively small compared to the buoys and the complete field of wind-derived motions. AMSR-E is also affected by surface melt, but its summer errors are not as high as SSMI, likely due to the higher spatial resolution.

Of note also is that the wind-derived motion error statistics are comparable to the passive microwave estimates, even lower in many cases (especially summer). This indicates that winds should not necessarily be lower weighted than the other satellite sources. It also suggests that the product's use of an ice/wind speed ration of 1% is not unreasonable, though 2% may yield improvement, as shown in Table 4 of the main text.

This brief study indicates that the simplified values of C are not optimal. This presents an avenue to improve the combined motion product in a future version.

S2. Validation of combined motions with CRREL buoys

The combined daily motions are validated in the Arctic through comparison with independent buoys from the CRREL Ice Mass Balance Buoy program [*Perovich et al.*, 2020]. We compared estimates to 101 CRREL buoys from 2000-2016. The total number of buoy-combined motion observation pairs varied over 2000-2016, from a high of 3016 in 2007 to a low of 249 in 2002. A small number (<0.1%) of CRREL observations with erroneous velocities that were obviously too large were removed from the comparisons. Overall, there are a total of 25,392 pairs over the 17-year period, an average of 1494 per year. A map of the buoy tracks during 2015 is given in Figure S1 as an example of the coverage and the trajectories of buoy motions. In 2015, the year used for

the evaluation of the sensitivity of the wind-ice speed relationship, the 9 buoys resulted in a total of 2025 paired observations.

All of the CRREL buoy positions were converted to EASE grid coordinates and the u-component and v-component of velocity (relative to the EASE grid) was derived from the change in position over a 24-hour period. The combined gridded estimate closest to each CRREL buoy was selected for comparison; thus, each comparison was made generally within ~25 km. The results (Table S2) show that biases are around -0.1 cm/s for the u-component and around -0.66 to -0.69 cm/s for the v-component. Most notably, the biases were slightly reduced in Version 4, indicating that the improvements in processing do result in improved accuracy of the motions. Similarly, the error standard deviations are around 4 cm/s for both velocity components and Version 4 reduces this error by ~0.3 cm/s over Version 3.

A 2-dimensional histograms of the distributions of the errors relative to the CRREL buoys (Figure S2), shows more detailed error characterization. The largest number of buoy-combined motion pairs have differences < 1cm/s. Version 4 shows slightly more pairs within this range, indicating an improvement over Version 3, in agreement with the statistics in Table S2.

As noted in Section 2.1 of the main text on *Reanalysis winds*, for the wind forcing, we used a 1% scale factor for the ice speed relative to wind speed. Other assessments have shown that 2% may be more legitimate, especially in recent years with the observed positive trend in ice speed. To investigate the potential effect of underestimating ice speed from winds in our product, we compared the combined motion fields with both 1% and 2% scale factors to the 2015 CRREL buoy observations. There were a total of 2025 comparison for 2015. The results indicate little effect due to wind speed (Table S3), which is expected since the weighting of the wind-driven motion is lower than other sources. The comparison indicates that the magnitude of the bias changes little for the u-component, but actually increases for the v-component. The error standard deviations decrease, generally by ~0.5 cm/s. This suggests that 2% may indeed be an improvement, but the impact on the combined gridded is relatively small. Of course, the relationship between wind speed and ice motion is complicated and can be quite variable. It depends on the compactness of the ice cover, thickness, and wind direction relative to nearby coasts. We plan to investigate the

relationship further in the future, both regionally (for different sea ice conditions) and temporally (to investigate the effect of the long-term trend toward increasing speeds).

Table S1. Error estimates for selected periods from the source motion estimates. All values are in cm/s. The Number column indicates the total number of buoy-source matches used in the statistics. The bias columns given the average difference in the motion components (source minus buoy) and the SD diff column provides the standard deviation of the difference.

Year	Source	Season	Number	*u* bias	*v* bias	*u* SD diff	*v* SD diff
1985	SMMR	JFM	284	-0.18	0.06	3.66	3.39
1995	AVHRR	JFM	271	0.70	0.29	4.00	3.53
		JJA	80	-0.53	0.29	4.95	3.78
2005	AMSR-E	JFM	1195	-0.07	-0.20	3.78	3.68
		JJA	175	0.67	1.02	4.53	4.98
	SSMI 37	JFM	103	0.00	1.30	6.44	8.84
		JJA	93	-2.52	0.96	7.64	10.32
	SSMI 85	JFM	964	-0.05	0.16	4.57	4.53
		JJA	69	-2.07	3.67	6.79	9.14
	Wind	JFM	1254	0.48	0.73	4.36	5.13
		JJA	2101	0.55	0.72	4.15	4.45

Table S2. Validation statistics from comparison with CRREL buoys.

	***u*-component (cm/s)**	***v*-component (cm/s)**
Bias		
Version 3	-0.115	-0.687
Version 4	-0.111	-0.660
Error St. Dev.		
Version 3	4.20	4.32
Version 4	3.90	4.03

Table S3. Comparison with CRREL buoys of combined motions using different wind-speed scaling.

	***u*-component (cm/s)**	***v*-component (cm/s)**
Bias		
1% of wind speed	-0.267	-0.190
2% of wind speed	-0.263	-0.220
Error St. Dev.		
1% of wind speed	4.95	4.43
2% of wind speed	4.47	3.99

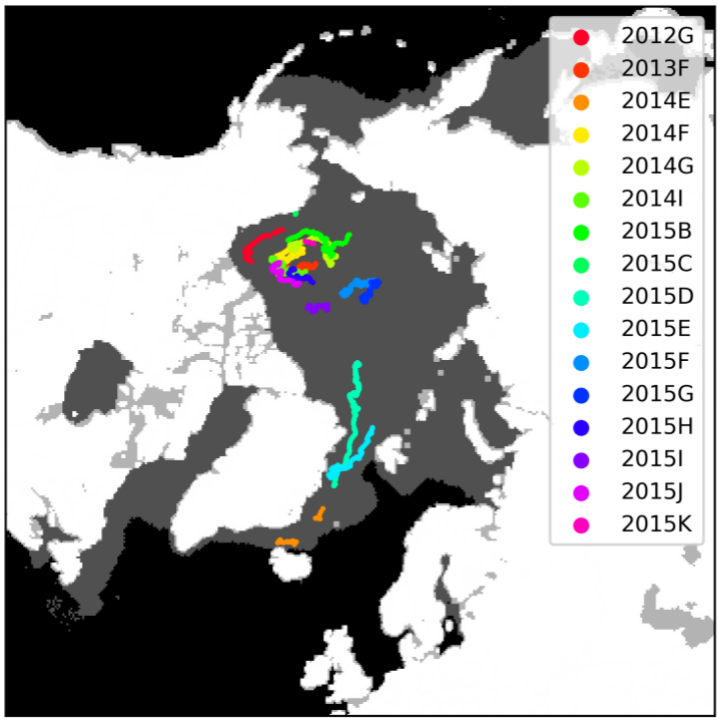

Figure S1. Map of CRREL buoy positions for 2015. The buoy IDs are color coded with the legend providing the CRREL buoy identifier; the year in the ID is the year of buoy deployment. All buoys that collected data during 2015 are shown except for buoys that were deployed on fast ice.

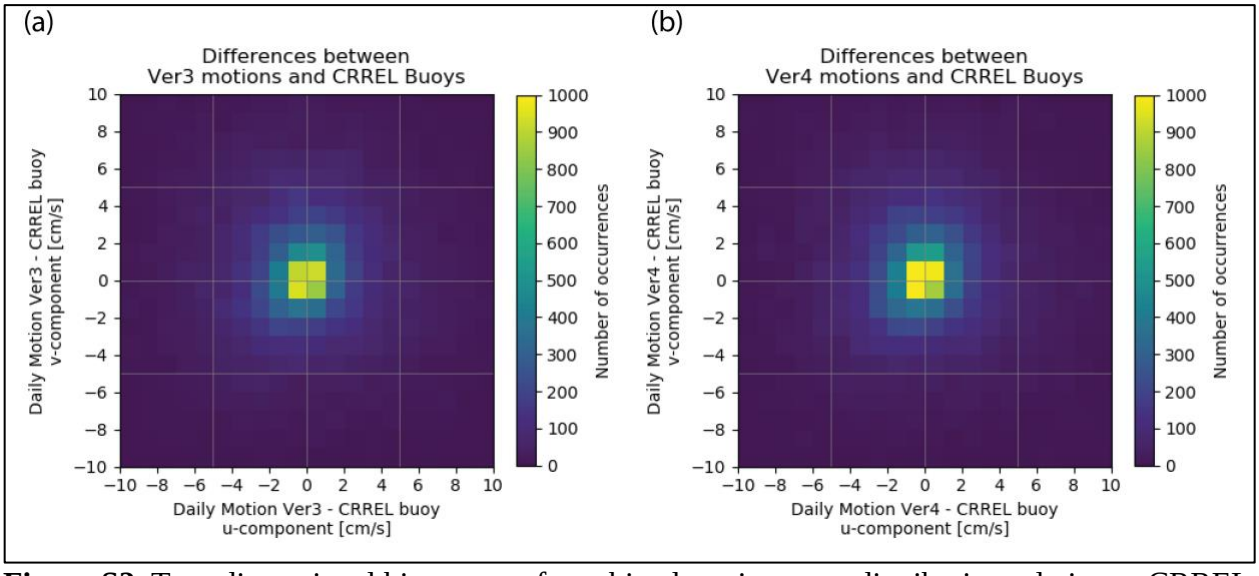

Figure S2. Two-dimensional histogram of combined motion error distribution relative to CRREL buoys for (a) Version 3 and (b) Version 4, binned into 1 cm/s increments. The *v*-component error is on the y-axis with the *u*-component error on the x-axis. The color scale indicates the number of occurrences within each bin.

Supplemental References

Perovich, D., J. Richter-Menge, and C. Polashenski, Observing and understanding climate change: Monitoring the mass balance, motion, and thickness of Arctic sea ice, http://imb-crrel-dartmouth.org/archived-data, 2020.